Genomic Psychiatry



OPEN

RESEARCH ARTICLE

The deubiquitinase OTULIN regulates tau expression and RNA metabolism in neurons

Karthikeyan Tangavelou¹ 📵, Virginie Bondu¹, Mingqi Li² 📵, Wei Li³ 📵, Francesca-Fang Liao² 📵, and Kiran Bhaskar^{1,4} 📵

The degradation of aggregation-prone tau is regulated by the ubiquitin-proteasome system and autophagy, which are impaired in Alzheimer's disease (AD) and related dementias (ADRD), causing tau aggregation. Protein ubiquitination, with its linkage specificity determines the fate of proteins, which can be either protein degradative or stabilizing signals. While the linear M1-linked ubiquitination on protein aggregates serves as a signaling hub that recruits various ubiquitin-binding proteins for the coordinated actions of protein aggregate turnover and inflammatory nuclear factor-kappa B (NF-kB) activation, the deubiquitinase OTULIN counteracts the M1-linked ubiquitin signaling. However, the exact role of OTULIN in neurons and tau aggregates clearance in AD are unknown. Based on our quantitative bulk RNA sequencing analysis of human inducible pluripotent stem cell-derived neurons (iPSNs) from an individual with late-onset sporadic AD (sAD2.1), a downregulation of the ubiquitin ligase activating factors (MAGE-A2/A2B/H1) and OTULIN long noncoding RNA (OTULIN lncRNA) was observed compared to healthy control WTC11 iPSNs. The downregulated OTULIN IncRNA is concurrently associated with increased levels of OTULIN protein and phosphorylated tau at p-S202/p-T205 (AT8), p-T231 (AT180), and p-S396/p-S404 (PHF-1) in sAD2.1 iPSNs. Inhibiting the deubiquitinase activity of OTULIN with a small molecule, UC495 reduced the phosphorylated tau in iPSNs and SH-SY5Y cells, whereas the CRISPR-Cas9-mediated OTULIN gene knockout (KO) in sAD2.1 iPSNs decreased both the total and phosphorylated tau levels. CRISPR-Cas9-mediated OTULIN KO in SH-SY5Y resulted in a complete loss of tau at both mRNA and protein levels, and increased levels of polyubiquitinated proteins, which are being degraded by the proteasome as confirmed with an inhibitor, Lactacystin. In addition, SH-SY5Y OTULIN KO cells showed downregulation of various genes associated with inflammation, autophagy, ubiquitin-proteasome system, and the linear ubiquitin assembly complex that consequently may prevent development of an autoinflammation in the absence of OTULIN gene in neurons. Together, our results suggest, for the first time, a noncanonical role for OTULIN in regulating the gene expression and RNA metabolism, which may have a significant pathogenic role in exacerbating tau aggregation in neurons. Thus, OTULIN could be a novel potential therapeutic target for AD and ADRD.

Genomic Psychiatry (2025), 1-11; doi: https://doi.org/10.61373/gp025a.0116

Keywords: Alzheimer's disease, tau, neurofibrillary tangles, LUBAC, OTULIN, M1-linked ubiquitin, autophagy, ubiquitin, proteasome, autoinflammation, RNA metabolism, RNA-binding proteins, RNA degradation

Introduction

The tau is encoded by the microtubule-associated protein tau or *MAPT* gene, which is located on chromosome 17q21 and expressed as six isoforms by alternative splicing in the human brain (1, 2). Tauopathy is a group of more than 20 neurodegenerative diseases, including Alzheimer's disease (AD), caused by intracellular aggregation of hyperphosphorylated tau as neurofibrillary tangles (NFTs) in neurons (3–5). Depending on the context in the neurons, tau can be a substrate of 20S proteasome, 26S proteasome, chaperone-mediated autophagy, microautophagy, macroautophagy, and aggrephagy, and their impaired degradative functions can lead to aggregation of tau as NFTs in tauopathy brains (reviewed elsewhere) (6, 7).

The linear ubiquitin assembly complex, LUBAC [Ring finger protein 31/HOIL-1-interacting protein (RNF31/HOIP), RanBP-type and C3HC4-type zinc finger-containing protein 1/Heme-oxidized IRP2 ubiquitin ligase 1 (RBCK1/HOIL-1) and SHANK-associated RH domain interactor (SHARPIN)] is the only known E3 ubiquitin ligase complex responsible for adding methionine1 (M1)-linked linear ubiquitin chains to protein aggregates (8). M1-linked ubiquitin is enriched around the nucleus and spread throughout the cell body of a neuron in various proteinopathies, including AD, frontotemporal dementia, Parkinson's disease (PD), polyglutamine (polyQ) diseases, and amyotrophic lateral sclerosis (8, 9). The ubiquitin chaperone, valosin-containing protein (VCP/p97 ATPase) recruits RNF31/HOIP to the sites of polyQ aggregates in Huntington's disease models for M1-linked polyubiquitination, which in turn recruits

autophagy receptors for efficient clearance of Huntingtin (Htt)-polyQ aggregates by autophagy (8). In another study, lysine48 (K48)-linked ubiquitination on tau aggregates is a prerequisite for recruiting VCP, which interacts with Heat Shock Protein (HSP70) to extract tau from aggregates for proteasomal degradation or extracellular secretion of seed-competent tau (10). Moreover, the tandem mass spectrometry analysis of tau-paired helical filaments (PHFs) isolated from the autopsy of human AD brains shows the presence of M1-linked polyubiquitin and various other ubiquitin-specific linkages, including K6-, K11-, K48-, and K63-linked ubiquitin chains (11–13).

In addition to recruiting autophagy receptors, the M1-linked ubiquitination on protein aggregates and host-invaded microbes is a signal for activation of nuclear factor-kappa B (NF- κ B), which regulates the transcription of DNA associated with immune response and cell survival under various stresses and infection (14–21). Most often, neuronally derived protein aggregates such as NFTs, α -synuclein, and Htt-polyQ become proinflammatory upon ubiquitination with M1-linked ubiquitin chains, which provide a binding platform to NF- κ B regulator/autophagy adaptor, NF- κ B essential modifier (NEMO), and autophagy receptors for NF- κ B activation and protein aggregate clearance, respectively (8, 9, 22, 23). Various other ubiquitin-specific linkages in NFTs recruit proteasome and aggrephagy machinery for tau clearance or extracellular secretion of seed competent tau upon impairment of proteostasis (6, 10).

The ovarian tumor (OTU) domain-containing deubiquitinase with linear linkage specificity (OTULIN) exclusively deubiquitinates interlinear

Corresponding Authors: Francesca-Fang Liao and Kiran Bhaskar, E-mail: fliao@uthsc.edu and kbhaskar@salud.unm.edu Received: 2 May 2025. Revised: 15 October 2025 and 28 October 2024. Accepted: 7 November 2025. Published online: 25 November 2025.



¹Department of Molecular Genetics and Microbiology, University of New Mexico Health Sciences Center, Albuquerque, NM 87131, USA; ²Department of Pharmacology, Addiction Science, and Toxicology, College of Medicine, University of Tennessee Health Science Center, Memphis, TN 38163, USA; ³Department of Pharmaceutical Sciences, College of Pharmacy, University of Tennessee Health Science Center, Memphis, TN 38163, USA; ⁴Department of Neurology, University of New Mexico Health Sciences Center, Albuquerque, NM 87131, USA



M1-linked ubiquitin chains except the peptide bond between target proteins and the first ubiquitin (24), whereas cylindromatosis (CYLD) deubiquitinates both M1- and K63-linked ubiquitin chains (25-27). Both the deubiquitinases, OTULIN and CYLD bind to HOIP/RNF31 and decrease the LUBAC-mediated M1-linked ubiquitination on target proteins and consequently decrease NF-kB activation under various inflammatory stimuli (28-32). Despite their role in negative regulation of NF-κB activity, OTULIN knockout (KO) showed increased levels of M1-linked ubiquitination on LUBAC components, RBCK1/HOIL-1 and SHARPIN, but not with CYLD KO, suggesting that OTULIN directly regulates LUBAC activity in basal condition (27). Moreover, OTULIN tyrosine56 (Y56) is essential for bonding with LUBAC component, HOIP/RNF31 to prevent TNF α -induced NF-κB activation, whereas phospho-OTULIN Y56 prevents interaction with HOIP and activates NF-κB (29, 33) In another study, OTULIN deubiquitinates LUBAC itself polyubiquitinated M1-linked linear chains, and prevents LUBAC-mediated cell death and inflammation (34).

Mice KO of HOIP (35), HOIL-1 (36), and OTULIN (34) genes are embryonic lethal, whereas SHARPIN deficiency causes chronic autoinflammatory disease in the skin of mice (37). Mutations in human HOIP L72P/Q399H (38, 39) and HOIL-1 deficiency (40) cause immunodeficiency and autoinflammation due to a lack of LUBAC-mediated M1-linked ubiquitination. Whereas mutations in human OTULIN Y244C/L272P/G281R decrease deubiquitinase activity, resulting in increased levels of M1linked polyubiquitination in patients with OTULIN-related autoinflammatory syndrome (41-43). The effect of OTULIN deficiency varies among cell types, such as in myeloid macrophages it causes elevated autoinflammation associated with increased M1-linked polyubiquitination and NF-B activity (42). OTULIN deficiency in lymphoid B or T cells causes no adverse inflammation due to complete loss of LUBAC components, HOIP, and SHARPIN at protein levels by proteasomal activity, but not their mRNAs levels (42). Despite OTULIN negatively regulates the M1-linked polyubiguitin and its associated autoinflammation in ORAS (41-43), OTULIN also functions as a negative and positive regulator of autophagy (44) and proteasomes (45), respectively. However, the role of OTULIN in neuron is largely unknown.

Here, we tested the hypothesis that stabilizing M1-linked polyubiquitination will reduce the levels of hyperphosphorylated tau by inhibiting M1-linked deubiquitinase activity of OTULIN and leading to the enhanced tau clearance by proteasome-, calpain- or autophagy-mediated degradation. However, results obtained significantly deviated from supporting this original hypothesis and suggests a novel noncanonical role of OTULIN in tau expression and RNA metabolism in neurons.

Results

sAD2.1 iPSNs downregulate $\it OTULIN$ lncRNA and ubiquitin ligase activating factor $\it MAGE$

We performed bulk RNA sequencing analyses in sporadic Alzheimer's disease (sAD2.1) induced pluripotent stem cell line (iPSC)-derived neurons (iPSNs) and healthy control WTC11 iPSNs to identify the differentially expressed genes and transcripts. The complete details of the RNA sequencing data, including the mapped region, sequence coverage, ready density, principal component analysis, Pearson correlation matrix, and significantly altered biological processes/pathways are shown in Supplementary Figures S1-S7 and Supplementary Tables S1-S2. The differentially expressed gene analyses obtained from the bulk RNA sequencing of sAD2.1 versus WTC11 iPSNs show that the expressions of 2390 and 2124 genes were upregulating and downregulated significantly in sAD2.1 iPSNs, respectively compared to WTC11 (Figure 1A and B). Similarly, 3828 and 1852 RNA transcripts were up and downregulated, respectively in sAD2.1 iPSNs (Figure 1C), which may likely indicate dysregulated RNA metabolism. Notably, the gene expression of OTULIN long noncoding RNA (IncRNA) derived from OTULIN divergent transcript (OTULIN-DT) was significantly downregulated (Figure 1D) that may influence the transcription of OTULIN gene. However, based on our quantitative bulk RNA sequencing analysis, the downregulated OTULIN-DT did not significantly upregulate the expression of OTULIN gene in sAD2.1 iPSNs (Figure 1D). Since pathological tau accumulate in sAD2.1 iPSNs (46), we analyzed whether there is any correlation between the gene expression of MAPT and MAPT lncRNA or MAPT antisense RNA (MAPT-AS). Our quantitative bulk RNA analysis shows no significant difference between the MAPT and MAPT-AS1 gene expression levels in sAD2.1 iPSNs (Figure 1D). As expected, there was a positive correlation between sAD2.1 with AD and tauopathies in gene set enrichment analyses (GSEA) (Figure 1E and F). Gene Ontology (GO) mapped > 2000 genes significantly altered to be associated with "protein-binding" as a major molecular functional pathway (Supplementary Figure S5). The heatmap for gene expression analyses shows that the ubiquitin ligase activating factor of the melanoma antigen gene (MAGE) family members, including MAGE-A2/A2B/H1 were downregulated in sAD2.1 iPSNs (Figure 1G). However, we do not know whether there is any correlation between the downregulated ubiquitin ligase activator factor, MAGE and pathological tau accumulation in sAD2.1 iPSNs, which is currently beyond the scope of current study.

sAD2.1 iPSNs show increased levels of OTULIN and phosphorylated tau, whereas inhibition of OTULIN deubiquitinase or deletion of *OTULIN* gene decreases phosphorylated tau levels

The bulk RNA sequencing revealed that the downregulated OTULIN lncRNA did not significantly affect the expression of OTULIN gene at mRNA levels in sAD2.1 iPSNs (Figure 1D). However, it is plausible that increased stability of OTULIN at protein levels is most likely due to downregulation of the ubiquitin ligase activating factor MAGE and can negatively influence the pathological tau clearance in sAD2.1 iPSNs (Figure 1G). We therefore performed Western blotting experiments to identify if there is any correlation between the level of OTULIN protein and tau pathology in sAD2.1 iPSNs. Surprisingly, the OTULIN protein level was significantly elevated in sAD2.1 than in WTC11 iPSNs (Figure 2A and B). In addition, tau phosphorylation at p-S199/p-S202/p-T205 (AT8), p-T231 (AT180), and p-S396/p-S404 (PHF-1) was also significantly elevated in sAD2.1 iPSNs (Figure 2A and B). It is conceivable that the elevated OTULIN deubiquitinase counteracts with M1-linked polyubiquitinated proteins and consequently may increase tau pathology, and inhibiting the deubiquitinase activity of OTULIN may alleviate tau pathology in sAD2.1 iPSNs.

To identify a small molecule that can inhibit the catalytic activity of OTULIN deubiquitinase, compounds in a drug-like library were docked to the OTULIN deubiquitinase catalytic center (PDB: 3ZNV) using the Schrodinger Molecular Modeling Suite. In silico docking of small molecules with the deubiquitinase OTULIN catalytic center identifies UC495 as a potential OTULIN deubiquitinase inhibitor (Figure 2C). To test the hypothesis that the inhibition of OTULTIN deubiquitinase might alleviate tau pathology, sAD2.1 iPSNs were treated with compound UC495 to inhibit OTULIN deubiquitinase activity and subsequently assessed hyperphosphorylation (Figure 2D). Inhibiting OTULIN deubiquitinase activity significantly reduced the level of phosphorylated tau at AT8 site, and modestly decreased PHF-1-positive tau levels compared to vehicle-treated sAD2.1 iPSNs (Figure 2D and E). However, neither OTULIN nor total tau levels were changed (Figure 2D and E).

Unlike pharmacological inhibition of OTULIN deubiquitinase activity with compound UC495, CRISPR-Cas9—mediated KO of *OTULIN* gene completely abolished its expression in sAD2.1 iPSNs (Figure 2F and G). As a result, both total and phosphorylated tau levels were significantly decreased in *OTULIN*-deficient sAD2.1 iPSNs (Figure 2F and G). The complete loss of tau in *OTULIN*-deficient sAD2.1 iPSNs intrigued us to investigate whether it is due to neuronal loss. We confirmed no adverse effect on neuronal differentiation despite the absence of both OTULIN and tau (Figure 2F and G). We also imaged the differentiated neurons using a bright field microscope, and found no significant morphological difference or alterations in neuronal marker, NeuN levels in *OTULIN*-deficient sAD2.1 iPSNs (Supplementary Figure S8). Together, these results suggest that CRISPR-Cas9—mediated *OTULIN* KO in sporadic sAD2.1 iPSNs causes complete loss of total tau and phosphorylated tau levels without affecting neuronal survivability.

Pharmacological inhibition of OTULIN deubiquitinase or deletion of OTULIN gene decreases tau in SH-SY5Y

In contrast to the effect of UC495 in reducing AT8 positive tau in sporadic sAD2.1 iPSNs (Figure 2F–G), inhibiting deubiquitinase activity of OTULIN with compound UC495 in human neuroblastoma cells, SH-SY5Y



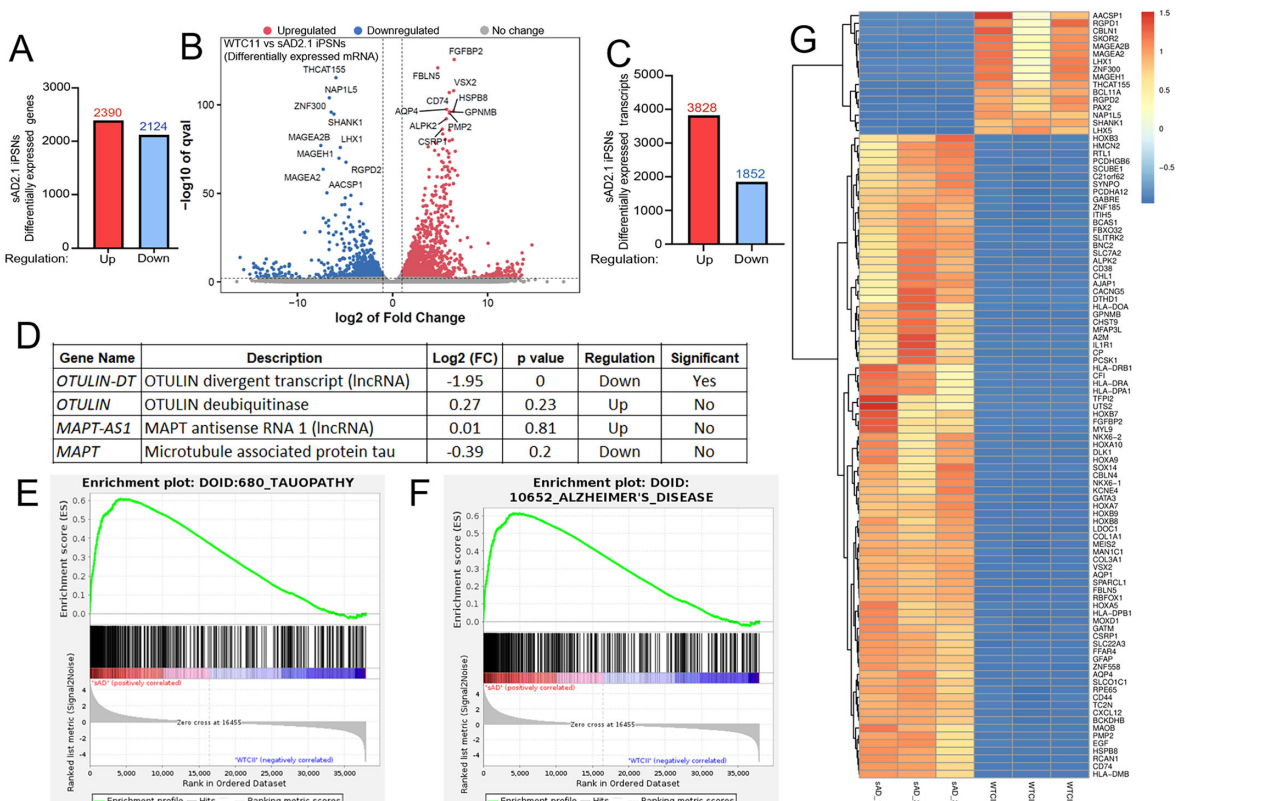


Figure 1. The sporadic Alzheimer's disease (sAD2.1) iPSC line-derived neurons (iPSNs) show significantly altered gene expression profile with increased OTULIN long noncoding RNA (OTULIN lncRNA) levels. (A) A comparative bulk RNA sequencing analysis of sAD2.1 vs WTC11 iPSNs shows upregulation of 2390 genes and downregulation of 2124 genes were differentially expressed in sAD2.1 iPSNs. (B) The volcano plot of differentially expressed genes in sAD2.1 iPSNs represents the log2 of fold change with a q value of < 0.05 as significant cutoff. On the plot, blue, red and gray dots indicate the levels of gene expression were downregulated, upregulated, and no changes, respectively. (C) sAD2.1 iPSNs shows altered RNA metabolism as reflected in the number of differentially expressed transcripts, with an upregulation of 3828 transcripts and downregulation of 1852 transcripts as compared to WTC11 iPSNs. (D) sAD2.1 iPSNs shows significant downregulation of OTULIN IncRNA (OTULIN-DT), which is inversely correlated with slightly upregulated OTULIN gene expression, which may exacerbate tau pathology. The MAPT gene expression may be slightly downregulated in contrast to either upregulated MAPT-AS1 or downregulated MAPT-IT1, which may initially function as a defense mechanism to prevent tau pathology progression in sAD2.1 iPSNs. (E, F) The gene set enrichment analyses (GSEA) pathways showing enrichment of signaling pathways relevant to tauopathy and Alzheimer's disease. (G) Heatmap analysis of differentially expressed genes in sAD2.1 (sAD_1,2,3) versus WTC11 (WTCII_1,2,3) iPSNs with three numbers from each group of cells. Heatmap intensity in color codes indicates upregulated (orange to red) and downregulated (blue) gene expression, respectively. Notably, the melanoma antigen gene (MAGE) family members (MAGE-A2/A2B/H1), which are known to enhance ubiquitin ligase activity, are significantly downregulated in sAD2.1 compared to WTC11 iPSNs.

significantly reduced OTULIN and total/phosphorylated (AT8, AT180, and PHF-1) tau levels (Figure 3A and B). Despite the reduction in endogenous tau levels, we did not observe cell toxicity as observed by the relatively uniform level of actin between UC495-treated and control SH-SY5Y cells (Figure 3A).

Like the pharmacological inhibition of OTULIN deubiquitinase with compound UC495, the CRISPR-Cas9-mediated gene interfering with OTULIN sgRNA completely abolished the OTULIN protein expression in SH-SY5Y (Figure 3C and D). Interestingly, knocking out of OTULIN gene in SH-SY5Y caused a complete loss of tau (Figure 3D). Collectively, inhibiting deubiquitinase of OTULIN with small molecule UC495 or CRISPR-Cas9-mediated KO of OTULIN gene in SH-SY5Y cell line decreases OTULIN levels, which in turn significantly reduces total tau levels (Figure 3A-D).

We predicted that the absence of OTULIN protein expression in SH-SY5Y OTULIN KO might have enhanced the degradation of tau by proteostasis activity. To determine the proteostasis activity causing complete loss of tau, SH-SY5Y OTULIN KO cells were pretreated with protein translation inhibitor, cycloheximide (CHX) for 1 h and then incubated with various proteostasis inhibitors (Lactacystin for 20S proteasome, MG132 for 26S proteasome, Bafilomycin A1 or Baf A1 for autophagy, and PD 150606 for Calpains 1 and 2) individually or together for an additional 4 h. The absence of deubiquitinase OTULIN in SH-SY5Y increased the accumula-

tion of polyubiquitinated proteins, which are actively being degraded by the proteasome as confirmed with the 20S proteasome inhibitor, Lactacystin, but not with the 26S proteasome inhibitor, MG132 at 10 or 20 μM concentrations (Figure 3D and E). Notably, the dynamics of polyubiquitinated proteins accumulation or degradation by the ubiquitin-proteasome system is enhanced in OTULIN KO cells compared to SH-SY5Y wild-type (WT) cells as confirmed with or without CHX under various proteostasis inhibitors (Figure 3C-E). Inhibiting the proteostasis activity did not increase the level of either OTULIN or Tau in SH-SY5Y WT cells except with 20 μM MG132, which decreases tau levels by unknown mechanism (Figure 3C and E). Thus, we conclude that none of the proteostasis inhibitors restored tau level in OTULIN deficient SH-SY5Y cells (Figure 3D), which motivated us to investigate the presence of tau at MAPT mRNA level by real-time quantitative reverse transcription PCR (gRT-PCR) along with 18S ribosomal RNA (18s rRNA) as a housekeeping reference gene for normalizing qRT-PCR data. Surprisingly, the MAPT mRNA was undetectable in the OTULIN-deficient SH-SY5Y compared to the WT cell line (Figure 3F).

OTULIN may function as a master regulator of RNA metabolism and gene expression

To determine whether OTULIN deficiency has any global effects on the mR-NAs of other genes or whether it is specific to *MAPT* mRNA, we isolated



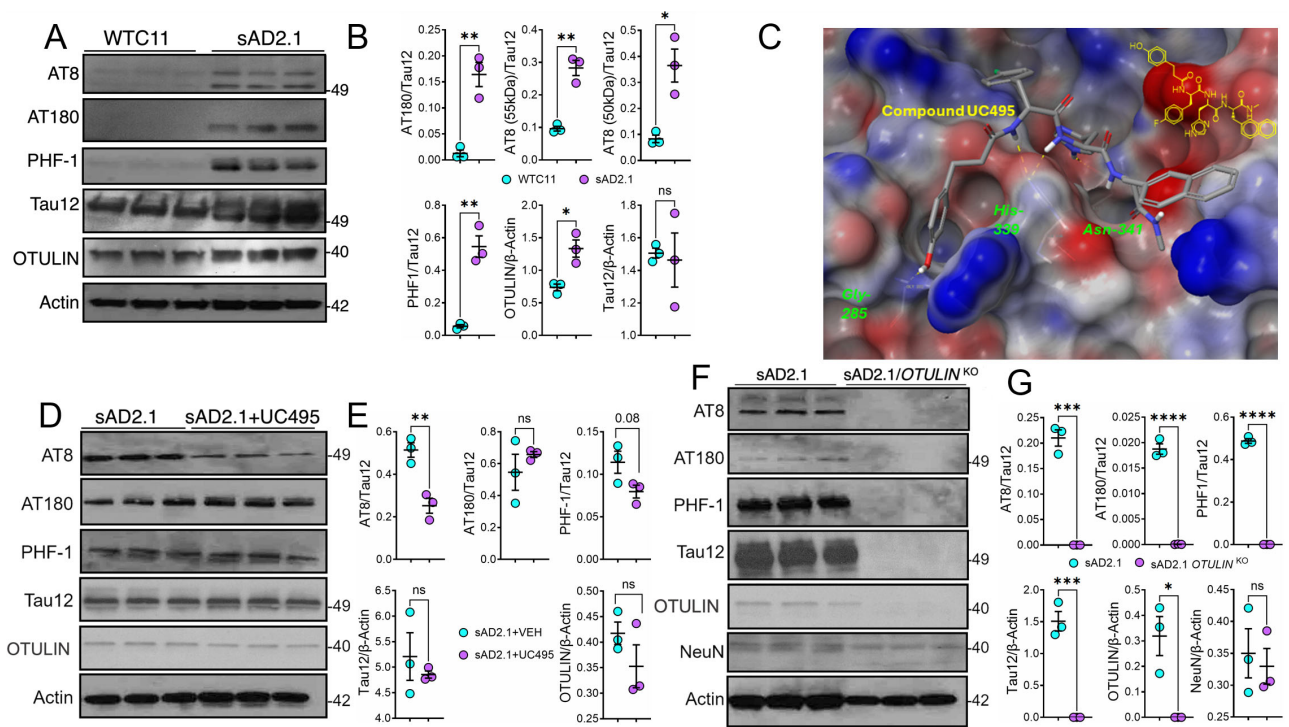


Figure 2. The sporadic sAD2.1 iPSNs increase the levels of OTULIN and phosphorylated tau, whereas inhibition of OTULIN deubiquitinase or deletion of OTULIN gene decreases phosphorylated tau levels. (A, B) OTULIN and phosphorylated tau levels were elevated in sporadic sAD2.1 iPSNs. Western blot analyses show significantly elevated phosphorylated tau at p-S199/p-S202/p-T205 (AT8), p-T231 (AT180), and p-S396/p-S404 (PHF-1) and OTULIN in sAD2.1 as compared to healthy control WTC11 iPSNs. (C) A Connolly surface representation of the major atoms of UC495 that interact with the OTULIN deubiquitinase binding pocket are shown in the figure. The OUTLIN surface is shown with electrostatic potentials, with red color indicating regions of high negative potential (electron-rich), blue color indicating regions of high positive potential (electron-poor), and other colors representing intermediate potentials. (D, E) Pharmacological inhibition of OTULIN deubiquitinase with compound UC495 selectively decreases phosphorylated tau at AT8 site in sAD2.1 iPSNs. Western blot analyses showed significantly decreased AT8⁺ tau and a modest reduction of PHF-1⁺ tau upon inhibition of OTULIN deubiquitinase with compound UC495 in sAD2.1 iPSNs. (F, G) CRISPR-Cas9-mediated knockout (KO) of OTULIN causes a complete loss of total tau in sporadic sAD2.1 iPSNs. Western blot quantifications showing significantly reduced AT8, AT180, and PHF-1 positive as well as total tau in CRISPR-Cas9-mediated OTULIN KO of sporadic sAD2.1 as compared to sAD2.1 iPSNs. Note that the reduction is not due to toxicity to neurons, as no significant difference in the NeuN levels was noted. Data presented as mean + SEM; unpaired t test; *p < 0.05; **p < 0.01; ***p < 0.005; ****p < 0.001; n = 3.

total RNAs from SH-SY5Y OTULIN KO and WT cell lines, respectively and performed bulk RNA sequencing for differentially expressed mRNA profiling (Supplementary Tables S3 and S4 and Supplementary Figures S9-S12). A significant upregulation of 774 genes and downregulation of 13,341 genes in SH-SY5Y OTULIN KO compared to WT cell line were observed (Figure 4A and C). To further confirm that OTULIN regulates RNA metabolism, we performed RNA transcript analyses and identified significant upregulation of 1113 transcripts and downregulation of 43,003 transcripts in the OTULIN-deficient SH-SH5Y line (Figure 4B and D). To classify the differentially expressed genes belonging to specific functional characteristics, we performed a GO enrichment analysis, which showed differentially expressed genes are mainly associated with protein, nucleotide and RNA-binding functions, ribonucleoprotein complex, transferase activity, DNA repair, and mitochondrial proteins (Figure 4F and Supplementary Figure S13). The Kyoto Encyclopedia of Genes and Genomes (KEGG) cellular pathway enrichment analysis revealed that most of the differentially expressed genes belongs to RNA degradation, RNA polymerase, neurodegeneration, lysosome, autophagy, oxidative phosphorylation, nucleotide excision repair, and N-Glycan biosynthesis pathways (Figure 4G). Heatmap comparative analysis showed a few highly significant up (yellow, orange, and red) and downregulated (blue) gene expression in SH-SY5Y OTULIN KO and WT (Figure 4E). Notably, the tau encoding MAPT gene transcript is downregulated along with OTULIN interaction partners predicted by STRING protein-protein interaction network (Supplementary Figure S14 and Supplementary Table S5). Since OTULIN is a deubiquitinase and dysregulates RNA metabolism, we mainly focused on the expression level of ubiquitin-activating enzyme (E1), ubiquitin-conjugating enzyme (E2) and RNA-binding ubiquitin ligase enzyme (E3), and RNA decay/degradation factors. OTULIN deficiency downregulated ubiquitin B/C and upregulated E1 enzyme UBA3, many E2 conjugating enzymes, and RNA-binding ubiquitin ligases, RC3H2 and MEX3C (Supplementary Table S6). OTULIN KO also upregulated many RNA degradation/decay-associated proteins, heterogeneous ribonucleoproteins, and a few neurodegenerative disease-associated RNA-binding proteins (Supplementary Table S7). Details about mapped region, sequence coverage, ready density, principal component analysis, Pearson correlation matrix, and significantly altered biological processes/pathways are shown in Supplementary Figures S9–S13 and Supplementary Tables S3 and S4.

Discussion

The canonical function of OTULIN is deubiquitinate the linear M1-linked ubiquitin chains such as to counteract the LUBAC (RNF31/HOIP, RBCK1/HOIL-1, and SHARPIN) E3-ubiquitin ligase, which is destabilized by deubiquitinating the linear M1-linked polyubiquitin on HOIL-1 and SHARPIN. The deubiquitinase OTULIN functions as a negative regulator of LUBAC and M1-linked ubiquitin chains-associated NF-κB and autophagy. Since OTULIN is an M1-linked deubiquitinase, we anticipated that inhibiting its deubiquitinase activity in neurons would favorably stabilize the M1-linked ubiquitin chains on tau aggregates and clear the aggregates by proteasome- or autophagy-mediated degradation. However, we



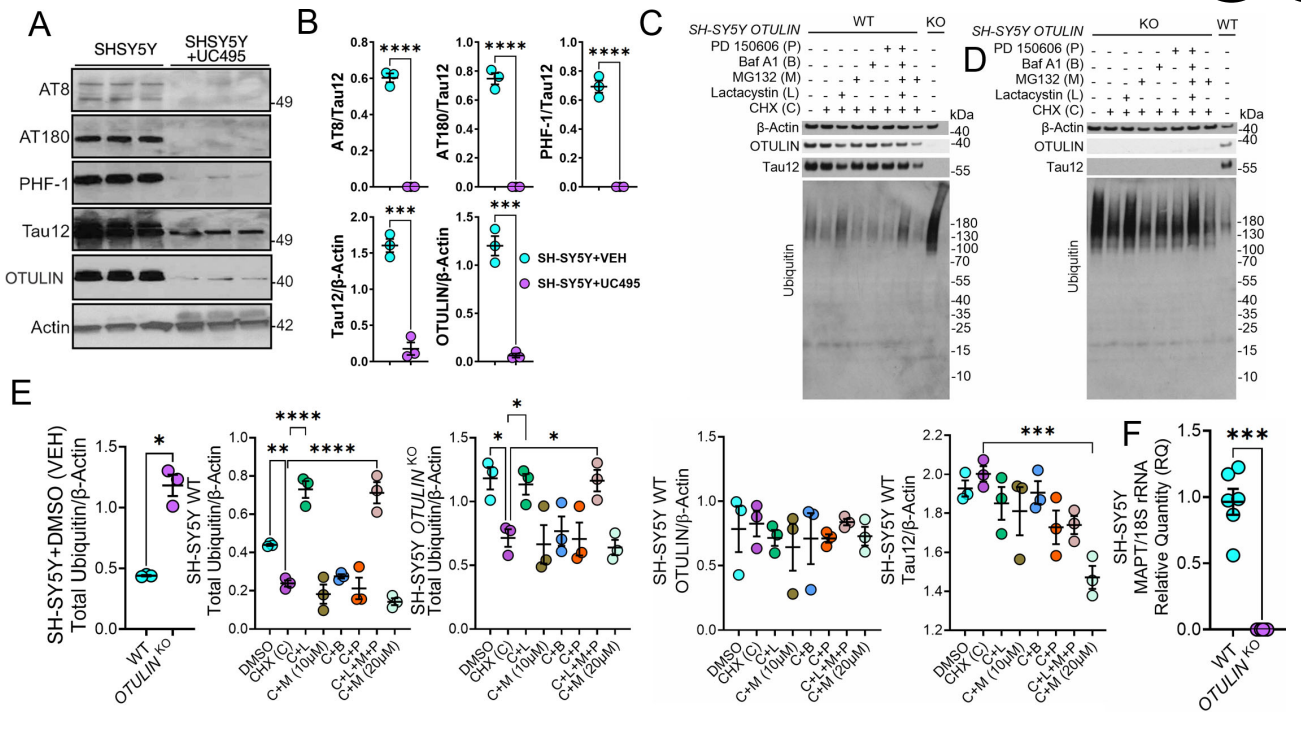


Figure 3. Pharmacological inhibition of OTULIN deubiquitinase or deletion of *OTULIN* gene decreases tau levels in human neuroblastoma cell line, SH-SY5Y. (A,B) Pharmacological inhibition of OTULIN with UC495 compound significantly decreases the levels of hyperphosphorylated and total tau, and OTULIN in SH-SY5Y cells. Western blot quantifications show significantly reduced AT8, AT180 and PHF-1 positive tau as well as total tau upon inhibition of OTULIN deubiquitinase with UC495 compound in SH-SY5Y cells as compared to DMSO-treated control. Inhibiting the deubiquitinase activity of OTULIN with UC495 also decreases the OTULIN levels. (C-E) CRISPR-Cas9-mediated *OTULIN* KO in SH-SY5Y causes a complete loss of tau and an accumulation of polyubiquitinated proteins. To study the dynamics of protein degradation in SH-SY5Y WT (C) and *OTULIN* KO (D) cells, protein translation was inhibited with 50 μM cycloheximide (CHX) 1 h prior adding the proteostasis inhibitors, 10 or 20 μM MG132 (26S proteasome), 10 μM Lactacystin (20S proteasome), 100 nM Bafilomycin A1 (Baf A1, autophagy), 100 μM PD 150606 (calpain 1/2) either individually or all four inhibitors together for 4 h. None of the inhibitors stabilizes tau in the absence of OTULIN (D) or change the OTULIN and Tau levels in wild-type cells except with 20 μM MG132, which decreases tau levels (C, E). (F) OTULIN deficiency in SH-SY5Y downregulates the transcription of *MAPT* gene. The real-time quantitative reverse transcription PCR (qRT-PCR) analysis shows the absence of *MAPT* mRNA in *OTULIN* KO compared to wild type SH-SY5Y. 18S ribosomal RNA (18s rRNA) was used as a housekeeping reference gene for normalizing qRT-PCR data (F). Data presented as mean + SEM; unpaired *t* test for comparing the two groups; Multiple comparisons were done by one-way ANOVA with Dunnett's multiple comparisons test; **p < 0.01; ***p < 0.005; ****p < 0.001; n = 3 to 6. Note that one of WT and *OTULIN* KO samples were loaded in blots in C and D (right most lanes) to control for samples r

surprisingly identified a complete loss of tau expression in *OTULIN* gene KO and explored an unappreciated noncanonical role of OTULIN in tau expression and RNA metabolism/gene expression in neurons.

Protein ubiquitination is a three-step posttranslational modification that requires the sequential action of three enzymes: ubiquitin-activating enzyme (E1), ubiquitin-conjugating enzyme (E2), and ubiquitin ligase enzyme (E3) (47) (Figure 5). However, protein ubiquitination becomes complex when decoding the functions of differential ubiquitination on the same protein with various linkages, such as M1-, K6-, K11-, K27-, K29-, K33-, K48-, and K63-linked ubiquitin chains. It also adds further complexity to understand the roles of homotypic, heterotypic, linear, and branched ubiquitination with various linkages on the same protein (6, 48). Such a complex ubiquitination occurs on the pathological tau aggregates in the brains of patients with tauopathies. Notably, prior studies have suggested that PHFs from human postmortem AD brains show M1-, K6-, K11-, K48-, and K63-linked ubiquitin chains via mass spectrometry (6, 11-13). Tau has been shown as a substrate of 20S proteasome, 26S proteasome, chaperone-mediated autophagy, microautophagy, macroautophagy, and aggrephagy depending on the posttranslational modifications, suggesting that ubiquitin can modify tau function and its half-life depends on the cellular contexts (6). However, it is unclear why tau requires differential ubiquitination to undergo degradation. Most likely, the sequential failure of various proteostasis machinery adds differential linkages of ubiquitin chains, such as K63- and M1-linked polyubiquitin, which

recruit ubiquitin-binding adaptors or receptors to activate the transcription factors. These factors, in turn, trigger gene expression for cell survival, immune responses, and the replenishment of proteostasis machinery for efficient clearance of protein aggregates (6, 8, 9, 22, 23).

The LUBAC is composed of RNF31/HOIP, RBCK1/HOIL-1, and SHARPIN, which function as an E3-ubiquitin ligase for M1-linked polyubiquitination on protein aggregates associated with various neurodegenerative diseases (8). The deubiquitinase OTULIN specifically deubiquitinates M1linked ubiquitin chains, such as those found in HOIL-1 and SHARPIN, whereas CYLD deubiquitinates both M1- and K63-linked ubiquitin chains but not the LUBAC (24-27). OTULIN functions as a negative regulator of LUBAC, NF-kB, and autophagy (8, 9, 22, 23). We, therefore, aimed to understand the role of OTULIN in clearance of tau aggregates in AD. We utilized healthy control WTC11 and sporadic AD2.1 human iPSC line-derived neurons (sAD2.1 iPSNs), and human neuroblastoma SH-SY5Y WT/OTULIN KO lines as model systems to understand the role of OTULIN in tau clearance and differential gene expressions. Our first RNA sequencing analyses of WTC11 and sAD2.1 iPSNs indicated that over 4000 genes and transcripts are differentially expressed in sporadic sAD2.1 iPSNs compared to healthy control WTC11 iPSNs (Figure 1A-C). The most notable hits are the melanoma antigen gene (MAGE) family members, including MAGEA2/A2B/H1, which are known to positively regulate the ubiquitin ligase activity of RING domain proteins (49). The MAGE family members, MAGE-A2/A2B/H1 are significantly downregulated in sAD2.1 iPSNs



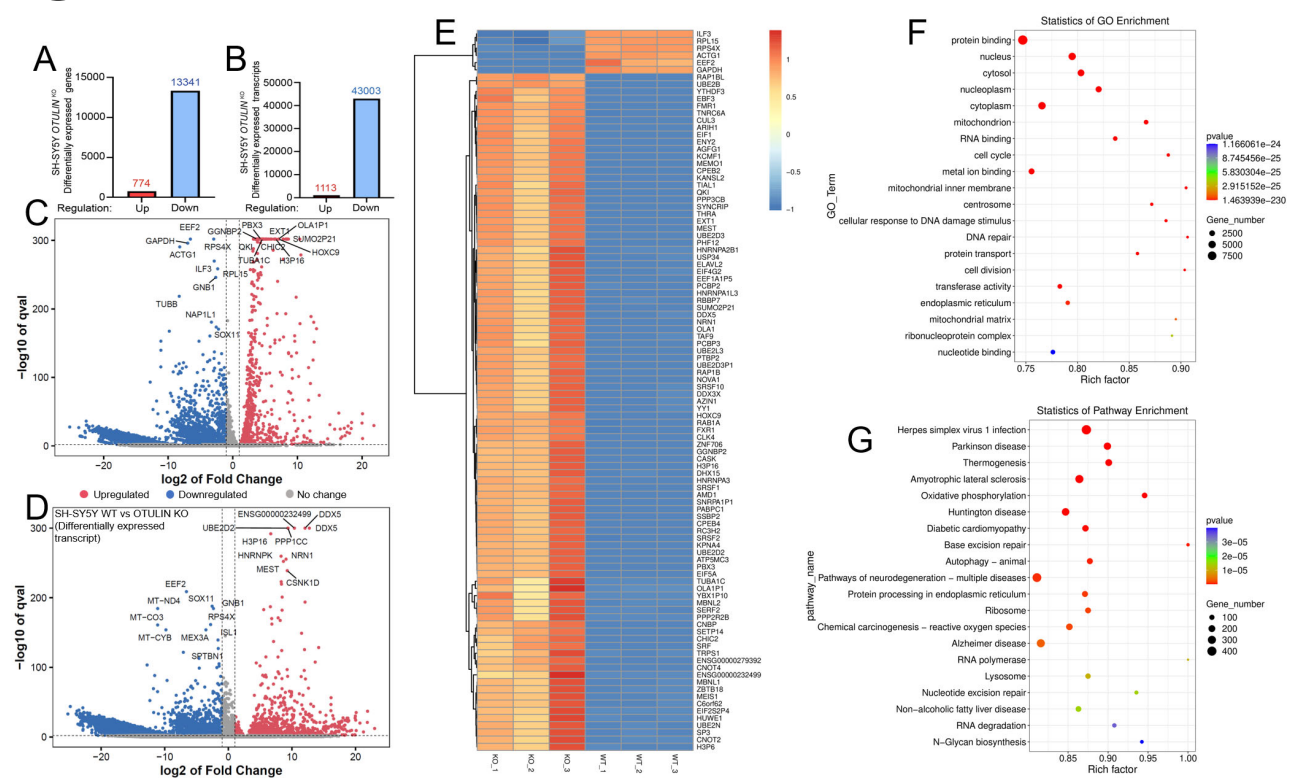


Figure 4. Dysregulated gene expression and RNA metabolism in SH-SY5Y *OTULIN* KO reveals a potential non-canonical role of OTULIN, which may serve as a master regulator of gene expression and RNA metabolism in neurons. (A) Bulk RNA sequencing analysis of *SH-SY5Y OTULIN* KO shows upregulation of 774 genes and a downregulation of 13,341 genes compared to wild type (WT), with three replicates from each group. (B) *OTULIN* gene deficiency dysregulates RNA metabolism in SH-SY5Y as reflected in the number of differentially expressed transcripts, with a downregulation of 43,003 transcripts and an upregulation of 1,113 transcripts compared to WT. (C) The volcano plot of differentially expressed genes in SH-SY5Y *OTULIN* KO represents the log2 of the fold change with a q value of < 0.05 as the significant cutoff. On the plot of log2 of fold changes, red dots at positive and blue dots at negative zones represent upregulated and downregulated gene expression, respectively. Whereas gray dots at the neutral zone denote no significant change of gene expression in both WT and KO lines. (D) The volcano plot of differentially expressed transcripts represents the log2 of fold change with a q value of < 0.05 as the significant cutoff for upregulated (red dots) or downregulated (blue dots) and no change (gray) of transcript levels in *OTULIN* KO as compared to WT. (E) Heatmap analysis of differentially expressed genes in *OTULIN* KO (KO_1,2,3) and wild type (WT_1,2,3) SH-SY5Y lines. Heatmap intensity in color codes indicates upregulated (orange to red) and downregulated (blue) gene expression, respectively. Most of the upregulated gene expressions in *OTULIN* KO are linked with mRNA degradation/decay and splicing pathways. (F) A Gene ontology (GO) scatter plot represents a set of genes that are associated with protein-to-nucleotide binding and were significantly differentially expressed genes in *OTULIN* KO line. (G) The cellular pathway analysis using the Kyoto Encyclopedia of Genes and Genomes (KEGG) scatter plot describes th

(Figure 1G), suggesting a likely loss of a few unknown ubiquitin ligases activity, which may explain the elevated pathological tau levels in sAD2.1 iPSNs. However, the level of M1-linked LUBAC E3-ligase components, including HOIP, HOIL-1, and SHARPIN, were not significantly altered in sAD2.1 iPSNs. Since MAGEs interact with more than 50 RING-type E3 ubiquitin ligases (50), a link between MAGEs and impaired tau clearance in AD needs further investigation.

Interestingly, a significant downregulation of OTULIN lncRNA is detected in sAD2.1 iPSNs (Figure 1D), which negatively correlated with elevated OTULIN protein levels. Since lncRNAs are intronic (51), overlapping, or antisense to protein-coding mRNAs (exons) like microRNAs, the downregulated OTULIN lncRNA may likely increase the level of OTULIN expression in sAD2.1 iPSNs. In a previous study, we observed an inverse correlation between elevated mRNA and reduced lncRNA or circular RNA (52). Notably, increased OTULIN is positively correlating with elevated levels of total tau and phosphorylated tau at AT8 (p-S202/p-T205), AT180 (p-T231), and PHF-1 (p-S396/p-S404) epitopes (Figure 2A and B), suggesting that OTULIN may regulate tau pathology.

To understand the role of the M1-linked deubiquitinase activity of OTULIN in tau pathology, we treated the sporadic sAD2.1 iPSNs with compound UC495. Inhibiting the OTULIN deubiquitinase with UC495

decreases phosphorylated tau at the AT8 epitope, but not at the AT180 and PHF-1 epitopes or total tau levels. Notably, inhibiting the deubiquitinase activity of OTULIN does not affect the level of OTULIN in sAD2.1 iPSNs, suggesting that inhibiting OTULIN deubiquitinase alone is sufficient to prevent tau pathology moderately (Figure 2D and E). However, the exact mechanism by which phosphorylated tau at the AT8 epitope is decreased upon inhibiting the OTULIN deubiquitinase with UC495 is unknown. It is possible that the compound UC495 may promote partial clearance of pathological tau by restoring proteostasis activity, such as by enhancing the E3-ubiquitin ligase activity of LUBAC or by stabilizing M1linked ubiquitin chains on ATG13 (44), a key regulator of autophagosome initiation. Alternatively, OTULIN inhibition may also likely downregulate the activation of certain tau kinases, such as CDK5, GSK-3 β , and MAPK, or any protein kinases that phosphorylate tau at \$202 and T205 (AT8). In contrast to the effect of compound UC495 in sAD2.1 iPSNs, OTULIN inhibition with UC495 in SH-SY5Y WT cells significantly decreases OTULIN and total tau; consequently, phosphorylated tau was not detectable with AT8, AT180, and PHF-1 antibodies (Figure 3A and B). Although the effect of compound UC495 is inconsistent with cell types such as sAD2.1 iPSNs (1 μ M) and SH-SY5Y (2 μ M) most likely is due to concentration and cell type dependent, UC495 could be a potential therapeutic molecule (based on



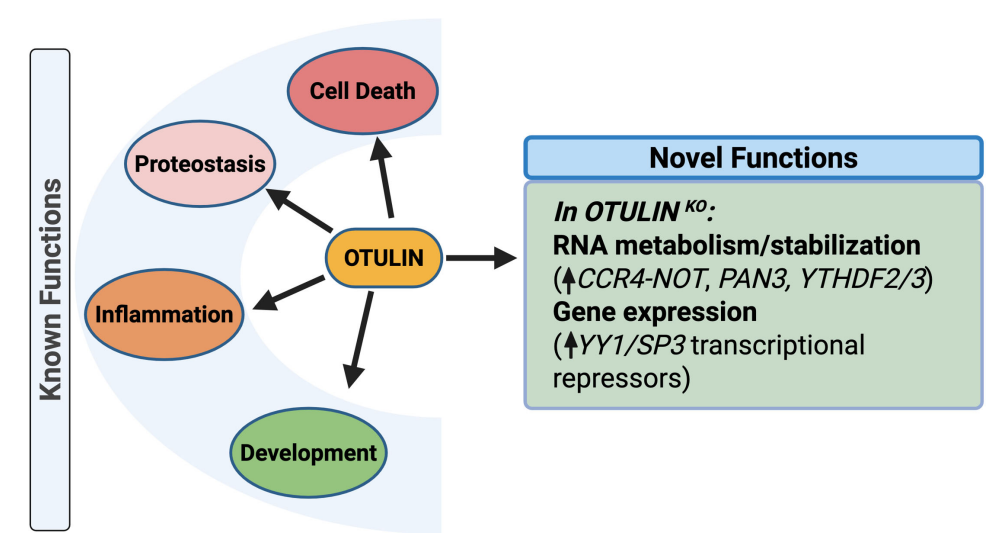


Figure 5. The working model shows the known and novel functions of OTULIN. OTULIN regulates proteostasis, cell death, inflammation, and cell survival/development. The novel non-canonical function identified in this study demonstrates OTULIN role as a regulator of RNA metabolism/stability and gene expression, including tau.

rather modulatory role than complete inhibition) that may alleviate tau pathology in tauopathy brains for future study.

To better understand the role of OTULIN in tau pathology, the OTULIN gene was knocked out in sAD2.1 iPSNs or the SH-SY5Y neuroblastoma line. We observed that the tau protein has completely blunted in its expression in both cell types with OTULIN KO (Figure 2F and G and Figure 3C and D). The overall morphology of sAD2.1 iPSNs was not affected in the absence of OTULIN (Supplementary Figure S8). However, it does exhibit morphological defects, including a lack of neurite-like projections, in the majority of SH-SY5Y OTULIN KO cells (Supplementary Figure S15). However, after 7-10 days in culture, the SH-SY5Y OTULIN KO cells were spontaneously differentiated into neuron-like cells without expressing tau (Supplementary Figures S15 and S16). We assumed that the loss of tau in SH-SY5Y OTULIN KO is due to enhanced proteostasis activity. We, therefore, used various proteostasis inhibitors with protein translation inhibitor, CHX, to understand the dynamics of tau degradation, including Lactacystin (20S proteasome), MG132 (26S proteasome), Bafilomycin-A1 (Baf-A1; autophagy), and PD 150606 (Calpains 1 and 2). Surprisingly, none of the proteostasis inhibitors stabilized tau (Figure 3D), which eventually motivated us to analyze MAPT mRNA levels by qRT-PCR, which suggests that MAPT mRNA has completely disappeared in the absence of OTULIN in SH-SY5Y line (Figure 3F). This finding further motivated us to perform bulk RNA sequencing to analyze whether the effects of OTULIN KO are specific to MAPT mRNA or dysregulated RNA metabolism globally.

Bulk RNA sequencing analysis revealed that SH-SY5Y OTULIN KO dysregulates RNA metabolism by downregulating the expression of 13,341 genes and 43,003 transcripts and upregulating 774 genes and 1113 transcripts, respectively, compared to SH-SY5Y WT (Figure 4A and B). It confirms that the effect of OTULIN KO is not specific to the downregulation of the MAPT gene. Still, it does globally and most likely function as a master regulator of RNA metabolism. However, the mechanism of OTULIN deficiency-associated dysregulated RNA metabolism is unknown. We, therefore, searched the possible candidates from our RNA sequencing data relevant to OTULIN-binding proteins, RNA metabolism associated with mRNA decay/degradation, mRNA stability, DNA transcription repressors, ubiquitination, and RNA-binding proteins. Primarily, we searched the differential expression of OTULIN-binding proteins obtained from the STRING protein-protein interactions database and identified that none of them were detectable at mRNA levels in our bulk RNA sequencing analysis, including the ubiquitin pathway-associated LUBAC components (HOIP, HOIL-1, SHARPIN), VCP, Ubiquitin B (UBB), and Ubiquitin C (UBC), and Neural Precursor Cell Expressed, Developmentally Down-Regulated 8 (NEDD8) (Supplementary Figure S14 and Supplementary Table S5).

Our RNA sequencing analysis showed that OTULIN KO in SH-SY5Y upregulated the expression of 774 genes and 1113 transcripts (Figure 4A and B), most likely required for cell survival under autoinflammation by suppressing gene transcription and accelerating RNA catabolism. We identified upregulation of ubiquitin-like modifier enzyme (UBA3), which is a component of NEDD8-activating enzyme 1 (NAE1), and its associated neddylation has been shown to be a regulator of neuronal aging and neurodegeneration in AD (53). Many ubiquitin-conjugating enzymes (UBE2s), including UBE2B/D2/D3/E3/H/K/L3/L5/M/N/Q1/V2/W were upregulated (Supplementary Table S6) among the approximately 40 E2 enzymes. However, many proteasome subunit genes were downregulated except proteasome activator subunit 3 (PSME3), proteasome 20S subunit beta 7 (PSMB7), proteasome 26S subunit, ATPase 6 (PSMC6), proteasome 26S subunit ubiquitin receptor, non-ATPase 2 (PSMD2), and proteasome 26S subunit, non-ATPase 14 (PSMD14) genes that were upregulated. Since more than 600 ubiquitin ligases (E3s) are involved in the ubiquitinproteasome pathway, we searched for RNA-binding ubiquitin ligases (54). We identified that most of them are downregulated except Ring finger and CCCH-type domains 2 (RC3H2) and Mex-3 RNA-binding family member C (MEX3C) (Supplementary Table S6), which are known to bind to 3 prime untranslated region (3'-UTR) of mRNAs, leading to deadenylation and degradation of mRNAs such as MHC-I mRNA (55). Interestingly, we identified that many mRNA stability regulator proteins encoding genes such as carbon catabolite repression 4-negative on TATA-less (CCR4-NOT) complex (CNOT) (56, 57), YTH N6-Methyladenosine RNA-binding protein F (YTHDF1/2/3), Poly(A) specific ribonuclease subunit 2 (PAN2), and PAN3 were either upregulated or downregulated in OTULIN KO cells (Figure 5 and Supplementary Table S7) that might have regulated mRNA stability or degradation depending on the context. In addition to accelerating mRNA degradation/decay, OTULIN KO may suppress DNA transcription globally by upregulating the expression of transcription factors such as Yin Yang 1 (YY1) and Specificity protein 3 (SP3), which are known to function as suppressors of gene expression (Figure 5 and Supplementary Table S7). It is conceivable from this interpretation that either the gene expression suppressors or mRNA stability regulators might have played an important role in the loss of tau expression in SH-SY5Y OTULIN KO cells. OTULIN KO also upregulates many heterogeneous ribonucleoproteins (HNRNPs) and neurodegenerative disease-associated RNA-binding proteins such as Fragile X messenger ribonucleoprotein 1 (FMR1), TAR DNA-binding protein (TARDBP/TDP-43), Ataxin 2 (ATXN2), and Musashi RNA-binding protein 1 (MSI1) (Supplementary Table S7). Since pathological tau is an inflammatory protein, it is plausible that knocking out of OTULIN gene in SH-SY5Y may hyperactivate LUBAC and stabilize



M1-linked linear ubiquitin chains causing autoinflammation, which in turn may negatively regulate LUBAC activity by down-regulating its components in addition to many thousands of genes, including tau to prevent developing an autoinflammation in neurons for cell survival.

In conclusion, sAD2.1 iPSNs showed elevated OTULIN and hyperphosphorylated tau. Inhibiting OTULIN deubiquitinase activity with UC495 has moderately decreased tau levels, whereas OTULIN KO has completely abolished tau expression at mRNA levels which indicates a possible novel, noncanonical role for OTULIN in RNA metabolism or gene expression, including those of tau. Notably, inhibiting the deubiquitinase OTULIN with UC495 in SH-SY5Y also decreased the level of OTULIN along with total tau which implies loss of deubiquitinase activity might have promoted OTULIN degradation, and eventually reduction in tau levels. Currently, we do not know whether it is regulated at the transcriptional level or at the translational level (RNA metabolism). Our quantitative bulk RNA sequencing analysis of SH-SY5Y OTULIN KO revealed a widespread change in the transcriptome and promoted neurite-like outgrowth spontaneously. The newly identified noncanonical role of OTULIN in neurons might function as a master regulator of RNA metabolism and gene expression, besides its canonical regulatory role of M1-linked deubiquitination of its target proteins. Therefore, while OTULIN could serve a potential drug target for AD/ADRD (Alzheimer's disease and related dementias), caution is warranted because of its pleotropic role in the CNS.

Methods

Cell culture

The WTC11 iPSCs (58) were a kind gift from Dr. Li Gan and sAD2.1 iPSCs (46) were obtained from Coriell. Neural progenitor cells (NPCs) of WTC11 and sAD2.1 were initially cultured in STEMdiff forebrain neuron differentiation kit (STEMCELL Technologies # 08600) and then matured in BrainPhys neuronal medium with SM1 supplement (STEMCELL Technologies # 05792). HEK293T cells were cultured in DMEM (Thermo Fisher Scientific # 11965092) and supplemented with 10% heat-inactivated fetal bovine serum (FBS) (Thermo Fisher Scientific # 16140071) and 2 mM L-Glutamine (Thermo Fisher Scientific # 25030081). All the cell cultures were maintained at 37°C with 5% $\rm CO_2$ and moisture. SH-SY5Y cells were grown in DMEM-F12 (1:1) (Thermo Fisher Scientific # 11320033) culture medium supplemented with 10% FBS and 1X concentration of penicillinstreptomycin (10,000 U/mL stock) (Thermo Fisher Scientific # 15140122) for UC495 treatment and $\it OTULIN$ KO.

CRISPR-Cas9-OTULIN single-guide RNA cloning

Targeting OTULIN single-guide RNA (sgRNA) sequences were obtained from the Genome-scale CRISPR Knock-OUT v2 libraries released by Dr. Feng Zhang Laboratory (59). The oligo nucleotide sequence of the target gene for Homo sapiens OTULIN gene is 5'-CGAGCGACCGCATGAGTCGG-3' and its reverse complement oligo nucleotide pair was cloned into the LentiCRISPRv2 as described here briefly. Each pair of Oligos (100 μ M) was mixed with T4 ligation buffer (NEB # B0202S; New England Biolabs) and nuclease-free ddH2O at 37°C for 30 min followed by 95°C for 5 min and cooled down to room temperature naturally to form double-stranded DNA fragments. A total of 5 μg of LentiCRISPRv2 (Addgene # 52961) was digested with restriction enzyme BsmBI in FastDigest buffer at 37°C for 30 min. Agarose gel-purified vectors were ligated with the above annealed oligonucleotide duplexes using ligase (NEB # M2200S). The resulting lenti-sgOTULIN plasmids were transformed into competent DH5α cells, which were selected by ampicillin to collect the positive clones for purifying the plasmid DNA carrying CRISPR-Cas9-OTULIN sgRNA.

Lentivirus production

The day prior to lentiviral transduction of sgRNA of OTULIN, HEK293T cells were plated onto a 6-well plate at a 70% confluency. A total of 60 μL (6 μg) of the sgRNA to OTULIN (sgOTULIN) plasmid (32) was added to 30 μL (3 μg) of psPAX packaging plasmid DNA and 15 μL (1.5 μg) of pvSvG envelope plasmid DNA in 345 μL of nuclease-free water with 50 μL of 2M CaCl2. The DNA mix was then added dropwise to 500 μL of 2x HBS buffer with slow vertexing and incubated at room temperature for 30 min. Then, the DNA mix solution was added to HEK293T cells and incubated at 37°C for overnight in a cell culture incubator. The culture medium was

changed 24 h later. The conditioned medium was harvested 48 h later and passed through a 0.2- μ m syringe filter. The lentivirus was then aliquoted and kept frozen at -80°C.

Lentivirus transduction of NPCs

Thawed Lentivirus (100 µL) was added to WTC11, and sAD2.1 NPCs were cultured in STEMdiff media onto a 6-well plate precoated with 200 μ L Geltrex (Thermo Fisher Scientific # A1569601). After overnight incubation, the lentivirus was aspirated and replaced with fresh growth medium. A 0.5 $\mu\text{g/mL}$ of puromycin (Thermo Fisher Scientific # J67236.XF) was added 48 h later for selection. After reaching a 70% confluency with puromycin, cells were transferred to a 6-well plate precoated with 10 μg Poly-L-Ornithine (Sigma # P4957-50ML) and 15 μg Laminin (Sigma # L6274-.5MG) and fed with BrainPhys neuronal medium (STEMCELL Technologies # 05790) for 20 days. Cells were then harvested and lysed in cold RIPA buffer (Thermo Fisher Scientific # 89901) with 1% Phenylmethylsulfonyl Fluoride (PMSF) (Sigma # 93482-50ML-F), 1X concentration of protease (Sigma # P8340-1ML) and phosphatase (Sigma # P2850-1ML) inhibitor cocktails. Lysates were spun down at 14,000 \times g for 20 min at 4°C. Lysates were transferred to new collection tubes and stored at $-80\ensuremath{^\circ\text{C}}$ for further analysis.

Inhibition of deubiquitinase OTULIN with compound UC495

The compound UC495 was originally identified through a virtual screening effort to identify small molecules of OTULIN deubiquitinase inhibitor and subsequently synthesized UC495. The compound UC495 was reconstituted in DMSO to make stock solution and kept at -20°C freezer until further use. Differentiated and fully matured sAD2.1 iPSNs were treated with 1 μM of UC495 overnight in a cell culture incubator. SH-SY5Y cells were treated with 2 μM of UC495 overnight, and DMSO (vehicle) alone treated cells as a control experiment. After overnight treatment with UC495, cells were washed with 1X PBS (1 mL/washing, three times) and harvested for Western blotting.

Bulk RNA sequencing and bioinformatics analysis

RNA was extracted from healthy control WTC11 iPSC line- and sporadic sAD2.1 iPSC line-derived neurons, and human neuroblastoma SH-SY5Y WT as control and SH-SY5Y OUTLIN KO, respectively. RNA was extracted with TRIzol reagent (Thermo Fisher Scientific # 15596026) and quantified by NanoDrop. A total of 2.0 mg of RNA was sent to LC Sciences and performed poly(A) RNA sequencing—sample quality control, library preparation, sequencing (150 bp PE, 6 GB data per sample), and analysis. De Novo assembly, alignment of RNA sequencing reads to reference genome, identification and construction of splice-junctions, report of known and novel transcripts with annotation and abundance, identification of alternate splicing and report of isoform abundance, test for differential expression at gene level and transcript level, GO and KEGG annotation and enrichment analysis GSEA were done by the LC Sciences. All raw RNA sequencing analysis data were deposited to NCBI Gene Expression Omnibus (GEO) with accession # GSE294290 (WTC11/sAD2.1 iPSNs) and # GSE294134 (SH-SY5Y WT/OTULIN KO).

Library construction and sequencing Poly(A) RNA sequencing library was prepared following Illumina's TruSeq-stranded-mRNA sample preparation protocol. RNA integrity was checked with Agilent Technologies 2100 Bioanalyzer. Poly(A) tail-containing mRNAs were purified using oligo-(dT) magnetic beads with two rounds of purification. After purification, poly(A) RNA was fragmented using divalent cation buffer in elevated temperature. The DNA library construction is shown in the following workflow. Quality control analysis and quantification of the sequencing library were performed using Agilent Technologies 2100 Bioanalyzer High Sensitivity DNA Chip. Paired-ended sequencing was performed on Illumina's NovaSeq 6000 sequencing system.

Transcripts assembly First, Cutadapt (60) and perl scripts in house were used to remove the reads that contained adaptor contamination, low quality bases and undetermined bases. Then sequence quality was verified using FastQC (http://www.bioinformatics.babraham.ac.uk/projects/fastqc/). We used HISAT2 (61) to map reads to the genome of ftp://ftp.ensembl.org/pub/release-112/fasta/homo_sapiens/dna/. The mapped



reads of each sample were assembled using StringTie (62). Then, all transcriptomes were merged to reconstruct a comprehensive transcriptome using perl scripts and gffcompare. After the final transcriptome was generated, StringTie (63) and ballgown (http://www.bioconductor.org/packages/release/bioc/html/ballgown.html) was used to estimate the expression levels of all transcripts.

Different expression analysis of mRNAs: StringTie (63) was used to perform expression level for mRNAs by calculating FPKM (fragments per kilobase of transcript per million mapped fragments). The mRNAs differential expression analysis was performed by R package DESeq2 (63) between two different groups [and by R package edgeR (64) between two samples]. The mRNAs with the parameter of false discovery rate below 0.05 and absolute fold change ≥ 2 were considered differentially expressed mRNAs. The following bioinformatics software was used to analyze the bulk RNA sequences: FastQC version 0.10.1 (Quality control), Cutadapt version 1.10 (Adapter remove), HISAT version 2.0 (Mapping), StringTie version 1.3.4 (Transcripts assembly), DESeq2/edgeR (Differential expression analysis), Perl scripts in house (GO and KEGG enrichment analysis), samtools version 0.1.19 (SNP/Indel analysis), ANNOVAR version 2017.09 (SNP/Indel annotation), and rMATS version 4.1.1 (Alternative splicing).

Real-time quantitative reverse transcription PCR

A total of 1.0 μq of purified RNA was diluted in RNAse free water to 25 μL as template for synthesizing complementary deoxyribonucleic acid (cDNA). The high capacity cDNA reverse transcription kit (Thermo Fisher Scientific # 4374966) was used to synthesize cDNA. A total of 25 μ L (1 $\mu\text{g})$ of RNA was mixed with 25 μL of reverse transcription components, including 10X reverse transcriptase (RT) buffer (5 μ L), 100 mM dNTP mix (2 μ L), 10X RT random primers (5 μ L), and MultiScribe RT (2.5 µL). The reaction mixture was incubated in a PCR machine by programming the temperature condition at 25°C for 10 min, 37°C for 120 min, and 85°C for 5 min. The resulting cDNA was used as a template to quantify the levels of target gene expression by the real-time qRT-PCR using Applied Biosystems StepOnePlus Real-Time PCR System with the software 2.3 version. A 25 μL of real-time qRT-PCR mixture was prepared with 12.5 µL TaqMan universal PCR mix, 1.25 µL gene target primer, 2.5 μ L cDNA, and 8.75 μ L RNAse free water. The reaction mixture in a 96-well plate was kept in the machine and the program was set to amplify and quantify the target gene at the specified temperature of 50° C for 2 min and 95°C for 10 min as predenaturation and followed by 40 cycles at 95°C for 15 s and 60°C for 1 min. The following TagMan gene expression assay primers were used from Thermo Fisher Scientific: Homo sapiens MAPT (TaqMan assay ID: Hs009021944_ml) as target gene, and eukaryotic 18S rRNA as housekeeping gene (Catalog no. 4319413E; Taq-Man assay ID: Hs99999901_s1).

Proteostasis inhibitors treatment and Western blotting

Human neuroblastoma SH-SY5Y WT/OTULIN KO cells (0.1 imes 10 6) were seeded in a 12-well plate. After overnight culturing of cells, protein translation was inhibited with 50 μM of CHX 1 h prior to adding the proteostasis inhibitors, 10 μ M MG132 (26S proteasome), 10 μ M Lactacystin (20S proteasome), 100 nM Bafilomycin A1 (Baf A1, autophagy), 100 μM PD 150606 (calpain 1/2) either individually or all four inhibitors together for 4 h. All the inhibitors were reconstituted with DMSO to prepare stock solutions and stored at -20° C until further use. After treatment, cells were washed with 1X PBS three times and lysed with ice-cold RIPA buffer with PMSF, protease, and phosphatase inhibitor cocktails and incubated on a rocker for 30 min at 4°C. Then the cell lysates were briefly sonicated on ice 20 kHz frequency for 30 s and centrifuged at 14,000 imes g for 10 min at 4°C. The protein concentration was quantified with the bicinchoninic acid assay kit (Thermo Fisher Scientific 23227) and measured the resulting purple-color intensity at 562 nm wavelength using the TECAN multimode microplate reader. The resulting supernatant was stored at -80° C or heat-denatured with 1X LDS-sample buffer (Thermo Fisher Scientific # NP0007) at 95°C for 10 min. Prior to loading the denatured samples onto a gel for protein separation, samples were centrifuged to collect the supernatant at 14,000 imes g for 5 min at 4°C. Western blots band intensities were quantified using ImageJ software. The level of β -Actin was used as

a loading control to normalize the resulting Western blots of protein of interest. The ratio of protein interest/ β -Actin levels were analyzed statistically using the GraphPad Prism software.

Proteostasis inhibitors and antibodies

The following proteostasis inhibitors were procured from Cayman Chemical. Cycloheximide (Cayman # 26924), Lactacystin (Cayman # 70980), MG132 (Cayman # 13697), Baf A1 (Cayman # 11038), and PD 150606 (Cayman # 13859). The following antibodies were procured from various vendors and their dilution mentioned here. β -Actin, Rb mAb (1:1000; Cell Signaling Technology # 4970S), OTULIN, Rb pAb (1:1000; Cell Signaling Technology # 14127S), Ubiquitin, Mo mAb (1:1000; Enzo Life Sciences # ENZ-ABS840), Tau12, Mo mAb (1:2000; Sigma # MAB2241), AT8, Mo mAb (1:8000; Thermo Fisher Scientific # MN1020), AT180, Mo mAb (1:8000, Thermo Fisher Scientific # MN1040), PHF-1 (1:10,000, a kind gift from Dr. Peter Davies), and NeuN (1:1500; GeneTex # GTX638922). Abbreviations: Mo – mouse; Rb – rabbit; mAb – monoclonal antibody; pAb – polyclonal antibody.

Data availability

The RNA sequencing data are available at NCBI GEO, with accession # GSE294290 (WTC11/sAD2.1 iPSNs) and # GSE294134 (SH-SY5Y WT/OTULIN KO). All other data are available from the corresponding author and shared upon a reasonable request.

Acknowledgments

We thank Dr. Li Gan, Weill Cornell Medical Center, for providing the WTC11 iPSC line. We also like to thank Dr. Orrin Myers for assisting with the generation of volcano plots with labels. Figure 5 was created in a licensed version of the 2024 BioRender® Program (www.biorender.com; accessed on 30 April 2025).

Author contributions

KB and FFL developed the project, acquired funding, and designed the experiment as well as oversaw the entire study. KB supervised KT and VB while FFL supervised ML. KT designed and conducted most of the experiments, analyzed the data, and wrote the manuscript. VB standardized and performed CRISPR-Cas9 KO experiments on iPSNs and performed Western blot analyses. ML and WL generated the CRISPR-Cas9 against *OUTLIN* and designed/characterized the UC495 compound. All authors take full responsibility for all data, figures, and text and approve the study's content and submission. No related work is under consideration elsewhere. All authors state that all unprocessed data are available, and all figures accurately present the original data. Corresponding authors: Professor KB for any aspect of the work except for UC495 and the CRISPR-Cas9 construct. Professor FFL for CRISPR-Cas9 construct and OTULIN antibodies. Professor WL for UC495. These corresponding authors take full responsibility for the submission process.

Funding sources

This research work was funded by the National Institutes of Health (NIH) funding: (1) RF1AG072703 (to FFL). (2) RF1NS083704-05A1, R01NS083704, New Mexico Higher Education Department – Technology Enhancement Fund (TEF), RF1AG072703-01A1, University of New Mexico (UNM) Health Sciences Center Bridge Funding, UNM Department of Molecular Genetics and Microbiology intradepartmental grant, the New Mexico Alzheimer's Disease Research Center (NM ADRC) P30 grant P30AG086404-01 funding (to KB); (3) UNM Center for Biomedical Research Excellence (CoBRE) in Center for Brain Recovery and Repair Pre-Clinical Core P20GM109089. Autophagy, Inflammation, and Metabolism (AIM) CoBRE Center P20GM121176-04. (4) A pilot development grant award from P30 parent grant P30AG086404-01 (to KT).

Author disclosures

The author(s) have confirmed that no conflict of interest exists.

References

- Wang Y, Mandelkow E. Tau in physiology and pathology. Nat Rev Neurosci. 2016;17(1):22–35. DOI: 10.1038/nrn.2015.1. PMID: 26631930
- 2. Buchholz S, Zempel H. The six brain-specific TAU isoforms and their role in Alzheimer's disease and related neurodegenerative dementia syndromes.



- Alzheimers Dement. 2024;20(5):3606–28. DOI: 10.1002/alz.13784. PMID: 38556838; PMCID: PMC11095451
- Grundke-Iqbal I, Iqbal K, Quinlan M, Tung YC, Zaidi MS, Wisniewski HM. Microtubule-associated protein tau. A component of Alzheimer paired helical Filaments. J Biol Chem. 1986;261(13):6084–89. PMID: 3084478
- 4. Bancher C, Brunner C, Lassmann H, Budka H, Jellinger K, Wiche G, et al. Accumulation of abnormally phosphorylated τ precedes the formation of neurofibrillary tangles in Alzheimer's disease. Brain Res. 1989;477(1–2):90–9. DOI: 10.1016/0006-8993(89)91396-6. PMID: 2495152
- Samudra N, Lane-Donovan C, VandeVrede L, Boxer AL. Tau pathology in neurodegenerative disease: disease mechanisms and therapeutic avenues. J Clin Invest. 2023;133(12):e168553. DOI: 10.1172/JCI168553. PMID: 37317972; PM-CID: PMC10266783
- Tangavelou K, Bhaskar K. The mechanistic link between tau-driven proteotoxic stress and cellular senescence in Alzheimer's disease. Int J Mol Sci. 2024;25(22):12335. DOI: 10.3390/ijms252212335. PMID: 39596399; PMCID: PMC11595124
- Jiang S, Bhaskar K. Degradation and transmission of tau by autophagicendolysosomal networks and potential therapeutic targets for tauopathy. Front Mol Neurosci. 2020;13:586731. DOI: 10.3389/fnmol.2020.586731. PMID: 33177989; PMCID: PMC7596180
- Well EMV, Bader V, Patra M, Sánchez-Vicente A, Meschede J, Furthmann N, et al. A protein quality control pathway regulated by linear ubiquitination. EMBO J. 2019;38(9):e100730. DOI: 10.15252/embj.2018100730. PMID: 30886048; PM-CID: PMC6484417
- 9. Furthmann N, Bader V, Angersbach L, Blusch A, Goel S, Sánchez-Vicente A, et al. NEMO reshapes the α -synuclein aggregate interface and acts as an autophagy adapter by Co-condensation with P62. Nat Commun. 2023;14(1):8368. DOI: 10. 1038/s41467-023-44033-0. PMID: 38114471; PMCID: PMC10730909
- Saha I, Yuste-Checa P, Da Silva Padilha M, Guo Q, Körner R, Holthusen H, et al. The AAA+ chaperone VCP disaggregates tau fibrils and generates aggregate seeds in a cellular system. Nat Commun. 2023;14(1):560. DOI: 10.1038/s41467-023-36058-2. PMID: 36732333; PMCID: PMC9894937
- Cripps D, Thomas SN, Jeng Y, Yang F, Davies P, Yang AJ. Alzheimer diseasespecific conformation of hyperphosphorylated paired helical filament-tau is polyubiquitinated through lys-48, Lys-11, and lys-6 ubiquitin conjugation. J Biol Chem. 2006;281(16):10825–38. DOI: 10.1074/jbc.M512786200. PMID: 16443603
- Abreha MH, Dammer EB, Ping L, Zhang T, Duong DM, Gearing M, et al. Quantitative analysis of the brain ubiquitylome in Alzheimer's disease. Proteomics. 2018;18(20):1800108. DOI: 10.1002/pmic.201800108. PMID: 30230243; PM-CID: PMC6283072
- Nakayama Y, Sakamoto S, Tsuji K, Ayaki T, Tokunaga F, Ito H. Identification of linear polyubiquitin chain immunoreactivity in tau pathology of Alzheimer's disease. Neurosci Lett. 2019;703: 53–57. DOI: 10.1016/j.neulet.2019.03.017. PMID: 30885635
- Iwai K, Fujita H, Sasaki Y. Linear ubiquitin chains: NF-κb signalling, cell death and beyond. Nat Rev Mol Cell Biol. 2014;15(8):503–8. DOI: 10.1038/nrm3836. PMID: 25027653
- Wijk SJLV, Fricke F, Herhaus L, Gupta J, Hötte K, Pampaloni F, et al. Linear ubiquitination of cytosolic Salmonella typhimurium activates NF-kb and restricts bacterial proliferation. Nat Microbiol. 2017;2(7):17066. DOI: 10.1038/nmicrobiol. 2017.66. PMID: 28481361
- Noad J, von der Malsburg A, Pathe C, Michel MA, Komander D, Randow F. LUBACsynthesized linear ubiquitin chains restrict cytosol-invading bacteria by activating autophagy and NF-κb. Nat Microbiol. 2017;2(7):17063. DOI: 10.1038/ nmicrobiol.2017.63. PMID: 28481331; PMCID: PMC5576533
- Spit M, Rieser E, Walczak H. Linear ubiquitination at a glance. J Cell Sci. 2019;132(2):jcs208512. DOI: 10.1242/jcs.208512. PMID: 30659056
- Jahan AS, Elbæk CR, Damgaard RB. Met1-Linked ubiquitin signalling in health and disease: inflammation, immunity, cancer, and beyond. Cell Death Differ. 2021;28(2):473–92. DOI: 10.1038/s41418-020-00676-w. PMID: 33441937; PMCID: PMC7862443
- Fuseya Y, Iwai K. Biochemistry, pathophysiology, and regulation of linear ubiquitination: intricate regulation by coordinated functions of the associated ligase and deubiquitinase. Cells. 2021;10(10):2706. DOI: 10.3390/cells10102706. PMID: 34685685; PMCID: PMC8534859
- Sasaki K, Iwai K. Role of linear ubiquitination in inflammatory responses and tissue homeostasis. Int Immunol. 2023;35(1):19–25. DOI: 10.1093/intimm/ dxac047. PMID: 36149813
- Gao L, Zhang W, Shi XH, Chang X, Han Yi, Liu C, et al. The mechanism of linear ubiquitination in regulating cell death and correlative diseases. Cell Death Dis. 2023;14(10):659. DOI: 10.1038/s41419-023-06183-3. PMID: 37813853; PM-CID: PMC10562472

- 22. Wu C-J, Conze DB, Li T, Srinivasula SM, Ashwell JD. Sensing of Lys 63-linked polyubiquitination by NEMO is a key event in NF-κb activation. Nat Cell Biol. 2006;8(4):398–406. DOI: 10.1038/ncb1384. PMID: 16547522
- Goel S, Oliva R, Jeganathan S, Bader V, Krause LJ, Kriegler S, et al. Linear ubiquitination induces NEMO phase separation to activate NF-κb signaling. Life Sci Alliance. 2023;6(4):e202201607. DOI: 10.26508/lsa.202201607. PMID: 36720498; PMCID: PMC9889916
- Keusekotten K, Elliott PR, Glockner L, Fiil BK, Damgaard RB, Kulathu Y, et al. OTULIN antagonizes LUBAC signaling by specifically hydrolyzing Met1linked polyubiquitin. Cell. 2013;153(6):1312–26. DOI: 10.1016/j.cell.2013.05. 014. PMID: 23746843; PMCID: PMC3690481
- Sun S-C. CYLD: a tumor suppressor deubiquitinase regulating NF-κb activation and diverse biological processes. Cell Death Differ. 2010;17(1):25–34. DOI: 10. 1038/cdd.2009.43. PMID: 19373246; PMCID: PMC5848464
- Colombo E, Horta G, Roesler MK, Ihbe N, Chhabra S, Radyushkin K, et al. The K63 deubiquitinase CYLD modulates autism-like behaviors and hippocampal plasticity by regulating autophagy and mTOR signaling. Proc Natl Acad Sci U S A. 2021;118(47):e2110755118. DOI: 10.1073/pnas.2110755118. PMID: 34782467: PMCID: PMC8617491
- Draber P, Kupka S, Reichert M, Draberova H, Lafont E, de Miguel D, et al. LUBAC-recruited CYLD and A20 regulate gene activation and cell death by exerting opposing effects on linear ubiquitin in signaling complexes. Cell Rep. 2015;13(10):2258–72. DOI: 10.1016/j.celrep.2015.11.009. PMID: 26670046; PMCID: PMC4688036
- Takiuchi T, Nakagawa T, Tamiya H, Fujita H, Sasaki Y, Saeki Y, et al. Suppression of LUBAC -mediated linear ubiquitination by a specific interaction between LUBAC and the deubiquitinases CYLD and OTULIN. Genes Cells. 2014;19(3):254–72. DOI: 10.1111/qtc.12128. PMID: 24461064
- Schaeffer V, Akutsu M, Olma MH, Gomes LC, Kawasaki M, Dikic IBinding of OTULIN to the PUB domain of HOIP controls NF-κb signaling. Mol Cell. 2014;54(3):349– 61. DOI: 10.1016/j.molcel.2014.03.016. PMID: 24726327
- 30. Jono H, Lim JH, Chen L-F, Xu H, Trompouki E, Pan ZK, et al. NF-κb is essential for induction of CYLD, the negative regulator of NF-κb. J Biol Chem. 2004;279(35):36171–74. DOI: 10.1074/jbc.M406638200. PMID: 15226292
- Newton K, Gitlin AD. Deubiquitinases in cell death and inflammation. Biochem J. 2022;479(10):1103–19. DOI: 10.1042/BCJ20210735. PMID: 35608338; PMCID: PMC9162465
- Li M, Li L, Asemota S, Kakhniashvili D, Narayanan R, Wang X, et al. Reciprocal interplay between OTULIN-LUBAC determines genotoxic and inflammatory NFκb signal responses. Proc Natl Acad Sci U S A. 2022;119(33):e2123097119. DOI: 10.1073/pnas.2123097119. PMID: 35939695; PMCID: PMC9388121
- Elliott PR, Nielsen SV, Marco-Casanova P, Fiil BK, Keusekotten K, Mailand N, et al. Molecular basis and regulation of OTULIN-LUBAC interaction. Mol Cell. 2014;54(3):335–48. DOI: 10.1016/j.molcel.2014.03.018. PMID: 24726323; PM-CID: PMC4017264
- Heger K, Wickliffe KE, Ndoja A, Zhang J, Murthy A, Dugger DL, et al. OTULIN limits cell death and inflammation by deubiquitinating LUBAC. Nature. 2018;559(7712):120–24. DOI: 10.1038/s41586-018-0256-2. PMID: 29950720
- Peltzer N, Rieser E, Taraborrelli L, Draber P, Darding M, Pernaute B, et al. HOIP deficiency causes embryonic lethality by aberrant TNFR1-mediated endothelial cell death. Cell Rep. 2014;9(1):153–65. DOI: 10.1016/j.celrep.2014.08.066. PMID: 25284787
- Peltzer N, Darding M, Montinaro A, Draber P, Draberova H, Kupka S, et al. LUBAC is essential for embryogenesis by preventing cell death and enabling haematopoiesis. Nature. 2018;557(7703):112–17. DOI: 10.1038/s41586-018-0064-8. PMID: 29695863; PMCID: PMC5947819
- Kumari S, Redouane Y, Lopez-Mosqueda J, Shiraishi R, Romanowska M, Lutz-mayer S, et al. Sharpin prevents skin inflammation by inhibiting TNFR1-induced keratinocyte apoptosis. Elife. 2014;3:e03422. DOI: 10.7554/eLife.03422. PMID: 25443631; PMCID: PMC4225491
- Boisson B, Laplantine E, Dobbs K, Cobat A, Tarantino N, Hazen M, et al. Human HOIP and LUBAC deficiency underlies autoinflammation, immunodeficiency, amylopectinosis, and lymphangiectasia. J Exp Med. 2015;212(6):939–51. DOI: 10.1084/jem.20141130. PMID: 26008899; PMCID: PMC4451137
- Oda H, Beck DB, Kuehn HS, Sampaio Moura N, Hoffmann P, Ibarra M, et al. Second case of HOIP deficiency expands clinical features and defines inflammatory transcriptome regulated by LUBAC. Front Immunol. 2019;10:479. DOI: 10.3389/fimmu.2019.00479. PMID: 30936877; PMCID: PMC6431612
- Krenn M, Salzer E, Simonitsch-Klupp I, Rath J, Wagner M, Haack TB, et al. Mutations outside the N-terminal part of RBCK1 may cause polyglucosan body myopathy with immunological dysfunction: expanding the genotype-Phenotype spectrum. J Neurol. 2018;265(2):394–401. DOI: 10.1007/s00415-017-8710-x. PMID: 29260357; PMCID: PMC5808061



- Zhou Q, Yu X, Demirkaya E, Deuitch N, Stone D, Tsai WL, et al. Biallelic hypomorphic mutations in a linear deubiquitinase define otulipenia, an early-onset autoinflammatory disease. Proc Natl Acad Sci U S A. 2016;113(36):10127–32. DOI: 10.1073/pnas.1612594113. PMID: 27559085; PMCID: PMC5018768
- Damgaard RB, Walker JA, Marco-Casanova P, Morgan NV, Titheradge HL, Elliott PR, et al. The deubiquitinase OTULIN is an essential negative regulator of inflammation and autoimmunity. Cell. 2016;166(5):1215–30.e20. DOI: 10.1016/j. cell.2016.07.019. PMID: 27523608; PMCID: PMC5002269
- Damgaard RB, Elliott PR, Swatek KN, Maher ER, Stepensky P, Elpeleg O, et al. OTULIN deficiency in ORAS causes cell type-specific LUBAC degradation, dysregulated TNF signalling and cell death. EMBO Mol Med. 2019;11(3):e9324. DOI: 10.15252/emmm.201809324. PMID: 30804083; PMCID: PMC6404114
- 44. Chu Y, Kang Y, Yan C, Yang C, Zhang T, Huo H, et al. LUBAC and OTULIN regulate autophagy initiation and maturation by mediating the linear ubiquitination and the stabilization of ATG13. Autophagy. 2021;17(7):1684–99. DOI: 10.1080/15548627.2020.1781393. PMID: 32543267; PMCID: PMC8354604
- Tao P, Wang S, Ozen S, Lee PY, Zhang J, Wang J, et al. Deubiquitination of proteasome subunits by OTULIN regulates type I IFN production. Sci Adv. 2021;7(47):eabi6794. DOI: 10.1126/sciadv.abi6794. PMID: 34797715; PMCID: PMC8604410
- Binder JL, Chander P, Deretic V, Weick JP, Bhaskar K. Optical induction of autophagy via transcription factor EB (TFEB) reduces pathological tau in neurons. PLoS One. 2020;15(3):e0230026. DOI: 10.1371/journal.pone.0230026. PMID: 32208437; PMCID: PMC7092971
- Komander D, Rape M. The ubiquitin code. Annu Rev Biochem. 2012;81(1):203–29. DOI: 10.1146/annurev-biochem-060310-170328. PMID: 22524316
- 48. French ME, Koehler CF, Hunter T. Emerging functions of branched ubiquitin chains. Cell Discov. 2021;7(1):6. DOI: 10.1038/s41421-020-00237-y. PMID: 33495455; PMCID: PMC7835216
- Doyle JM, Gao J, Wang J, Yang M, Potts PR. MAGE-RING protein complexes comprise a Family of E3 ubiquitin ligases. Mol Cell. 2010;39(6):963–74. DOI: 10.1016/j.molcel.2010.08.029. PMID: 20864041; PMCID: PMC4509788
- Lee AK, Potts PR. A comprehensive guide to the MAGE family of ubiquitin ligases. J Mol Biol. 2017;429(8):1114–42. DOI: 10.1016/j.jmb.2017.03.005. PMID: 28300603; PMCID: PMC5421567
- Mattick JS, Amaral PP, Carninci P, Carpenter S, Chang HY, Chen L-L, et al. Long non-coding RNAs: definitions, functions, challenges and recommendations. Nat Rev Mol Cell Biol. 2023;24(6):430–47. DOI: 10.1038/s41580-022-00566-8. PMID: 36596869; PMCID: PMC10213152
- 52. Jiang S, Maphis NM, Binder J, Chisholm D, Weston L, Duran W, et al. Proteopathic tau primes and activates interleukin- 1β via myeloid-cell-specific MyD88-and NLRP3-ASC-inflammasome pathway. Cell Rep. 2021;36(12):109720. DOI: 10.1016/j.celrep.2021.109720. PMID: 34551296; PMCID: PMC8491766
- Saurat N, Minotti AP, Rahman MT, Sikder T, Zhang C, Cornacchia D, et al. Genomewide CRISPR screen identifies neddylation as a regulator of neuronal aging and AD neurodegeneration. Cell Stem Cell. 2024;31(8):1162–74.e8. DOI: 10.1016/j. stem.2024.06.001. PMID: 38917806; PMCID: PMC11405001
- Cano F, Miranda-Saavedra D, Lehner PJ. RNA-binding E3 ubiquitin ligases: novel players in nucleic acid regulation. Biochem Soc Trans. 2010;38(6):1621–26. DOI: 10.1042/BST0381621. PMID: 21118137
- 55. Cano F, Bye H, Duncan LM, Buchet-Poyau K, Billaud M, Wills MR, et al. The RNA-binding E3 ubiquitin ligase MEX-3C links ubiquitination with MHC-I mRNA degradation: MHC-I regulation by an RNA-binding E3 ligase. EMBO

- J. 2012;31(17):3596–606. DOI: 10.1038/emboj.2012.218. PMID: 22863774; PMCID: PMC3433784
- Collart MA. The Ccr4-not complex is a key regulator of eukaryotic gene expression. Wiley Interdiscip Rev RNA. 2016;7(4):438–54. DOI: 10.1002/wrna.1332. PMID: 26821858; PMCID: PMC5066686
- Poetz F, Corbo J, Levdansky Y, Spiegelhalter A, Lindner D, Magg V, et al. RNF219 attenuates global mRNA decay through inhibition of CCR4-NOT complex-mediated deadenylation. Nat Commun. 2021;12(1):7175. DOI: 10. 1038/s41467-021-27471-6. PMID: 34887419; PMCID: PMC8660800
- Chen Xu, Li Y, Wang C, Tang Y, Mok S-A, Tsai RM, et al. Promoting Tau secretion and propagation by hyperactive P300/CBP via autophagy-lysosomal pathway in tauopathy. Mol Neurodegener. 2020;15(1):2. DOI: 10.1186/s13024-019-0354-0. PMID: 31906970: PMCID: PMC6945522
- Sanjana NE, Shalem O, Zhang F. Improved vectors and genome-wide libraries for CRISPR screening. Nat Methods. 2014;11(8):783–84. DOI: 10.1038/nmeth.3047. PMID: 25075903; PMCID: PMC4486245
- Martin M. Cutadapt removes adapter sequences from high-throughput sequencing reads. EMBnet J 2011;17(1):10. DOI: 10.14806/ej.17.1.200.
- Kim D, Langmead B, Salzberg SL. HISAT: a fast spliced aligner with low memory requirements. Nat Methods. 2015;12(4):357–60. DOI: 10.1038/nmeth.3317. PMID: 25751142: PMCID: PMC4655817
- Pertea M, Pertea GM, Antonescu CM, Chang T-C, Mendell JT, Salzberg SL. StringTie enables improved reconstruction of a transcriptome from RNA-seq reads. Nat Biotechnol. 2015;33(3):290–95. DOI: 10.1038/nbt.3122. PMID: 25690850; PMCID: PMC4643835
- Love MI, Huber W, Anders S. Moderated estimation of fold change and dispersion for RNA-seq data with DESeq2. Genome Biol. 2014;15(12):550. DOI: 10.1186/ s13059-014-0550-8. PMID: 25516281; PMCID: PMC4302049
- Robinson MD, McCarthy DJ, Smyth GK. edgeR: a bioconductor package for differential expression analysis of digital gene expression data. Bioinformatics. 2010;26(1):139–40. DOI: 10.1093/bioinformatics/btp616. PMID: 19910308; PMCID: PMC2796818

Publisher's note: Genomic Press maintains a position of impartiality and neutrality regarding territorial assertions represented in published materials and affiliations of institutional nature. As such, we will use the affiliations provided by the authors, without editing them. Such use simply reflects what the authors submitted to us and it does not indicate that Genomic Press supports any type of territorial assertions.

Open Access. This article is licensed to Genomic Press under the Creative Commons Attribution 4.0 International Public License (CC BY 4.0). The license requires: (1) Attribution — Give appropriate credit (creator name, attribution parties, copyright/license/disclaimer notices, and material link), link to the license, and indicate changes made (including previous modifications) in any reasonable manner that does not suggest licensor endorsement. (2) No additional legal or technological restrictions beyond those in the license. Public domain materials and statutory exceptions are exempt. The license does not cover publicity, privacy, or moral rights that may restrict use. Third-party content follows the article's Creative Commons license unless stated otherwise. Uses exceeding license scope or statutory regulation require copyright holder permission. Full details: https://creativecommons.org/licenses/by/4.0/. License provided without war-

ranties.